

# MODELING OF GRAVITY EFFECTS IN STREAMLINE-BASED SIMULATION FOR THERMAL RECOVERY <sup>\*)</sup>

by  
Usman

## ABSTRACT

*Gravity effects are more prominent in thermal recovery simulations due to larger density difference between phases. Historically, the streamline method has been unable to account for gravity effects. This is a result of assuming that the fluid path follows the streamline path and therefore no communication among streamlines. However with gravity, a fluid pathline is different from a fluid streamline. Each phase can move vertically as a result of the gravity segregation effect in addition to the flow along streamline.*

*Gravity effects are accounted in the streamline method by an operator splitting technique. The idea is to isolate the convective flow from diffusion due to gravity for separate solutions. The convective part is calculated along the common streamline trajectories and the diffusion part is determined by the direction of gravity. While this has been done successfully for isothermal problems, it is still a challenge to obtain both accuracy and efficiency for non-isothermal flow. This paper further examines the mixed streamline method with an operator splitting technique for this class of problems. The pressure equation for defining streamlines was derived by summing up the mass conservation equations. Then, the mass and heat transport equations in terms of the streamline time-of-flight coordinate were solved for each streamline. A gravity step will be followed by solving the segregation equations over the dimensional grid. For simplification of modeling, heat was assumed to transfer by convection only, of which direction is parallel with the flowing phases and the influence of temperature in the simulation model is through changes in fluid viscosity only. The proposed approach was tested through simulation of heavy oil recovery by means of hot waterflooding. The results were verified with those of a commercial fully implicit thermal simulator.*

*Key words: Thermal recovery, hot waterflooding, gravity effect, streamline simulator, operator splitting technique*

## I. INTRODUCTION

Nowadays, the streamline method is very popular and commonly applied in the reservoir simulation studies, nevertheless this technology has been in the literature since Muskat and Wyckoff's 1934 paper and has repeated attention since then. Streamline-based simulation is an attractive alternative to cell-based simulation because of the fundamentally different approach in moving fluids. Instead of moving

fluids from cell to cell, the streamline breaks up the reservoir into one-dimensional (1D) systems and approximates 3D fluid flow calculations by a sum of 1D solutions along streamlines. Transformation from a 3D problem to 1D systems is facilitated by the time-of-flight concept (Datta-Gupta and King, 1995, Pollock, 1988). Unfortunately, this concept limits the application of the streamline method to the convection problems only. The contribution of physical dif-

---

<sup>\*)</sup> This paper was selected for presentation by the JFES Program Committee following the review of abstract submitted by author(s).

fusion due to gravity, capillary force, and conduction cannot be solved using 1D streamline.

To account for multiphase gravity effects, one possibility is to trace a single set of streamlines along the total velocity vector and then use an operator splitting technique to correct for multiphase gravity effects. A similar operator splitting technique applied to front-tracking is used by Bratvedt, *et al.*, 1996. This technique was implemented in a number of streamline simulators to account for multiphase gravity effects (Batycky, 1997, Crane, *et al.*, 2000) and showed good achievements. Gravity was treated as an additional correction to the convective step along streamline. Additional processes such as capillary pressure can also be included in the streamline method by the same manner (Rodriguez, *et al.*, 2003).

The mixed streamline and operator splitting techniques in modeling a reservoir undergoing displacement process has been focused on the isothermal flow. This paper further examines this approach for non-isothermal flow. The coupling between mass and energy transport in thermal flood simulation adds considerable complexity. This then would be coupled with an appropriate thermodynamic formulation to account for changes in properties with temperature and pressure. In this paper, the mixed approach was applied to a simple problem of hot waterflooding formulation. Our interest is how good this mixed approach is to model the gravity effects in thermal displacements. Although simplified, the simulation demonstrates the main features of this strategy. We present the solution of the hot waterflooding simulation in 2D homogeneous and heterogeneous models and confirm the validity of the developed model by comparing with STARS, which is a commercial thermal reservoir simulator.

## II. GENERAL GOVERNING EQUATIONS

The governing equations for hot waterflooding based on the streamline method are first discussed. Then, we show the performance of the developed simulator to this particular problem.

### A. Hot Waterflooding Model

A mathematical model that describes hot waterflooding processes in heavy oil reservoirs is adopted from the two-phase black-oil model. The water and oil components are assumed to always exist in the water and oil phases. The governing equations for

the general thermal model, neglecting heat conduction, are given by:

$$-\nabla \cdot (\rho_w \vec{u}_w) + q_w \rho_w = \frac{\partial(\phi \rho_w S_w)}{\partial t} \quad (1)$$

$$-\nabla \cdot (\rho_o \vec{u}_o) + q_o \rho_o = \frac{\partial(\phi \rho_o S_o)}{\partial t} \quad (2)$$

$$\begin{aligned} &-\nabla \cdot (\rho_w H_w \vec{u}_w + \rho_o H_o \vec{u}_o) + q_w \rho_w H_w + q_o \rho_o H_o \\ &= \frac{\partial}{\partial t} (\phi (S_w \rho_w U_w + S_o \rho_o U_o) + (1-\phi) \rho_r C_r T) \end{aligned} \quad (3)$$

where the superscript w stands for the well conditions. The velocity,  $\vec{u}_\alpha$ , is given by Darcy's law,

$$\vec{u}_\alpha = -\frac{k k_{ra}}{m_a} (\tilde{N} p_a - r_a g \tilde{N} D) \quad a = w, o \quad (4)$$

The phase pressure is  $p_a$ ,  $D$  is the depth, and  $g$  is the gravitational constant. The volumetric flow rate per unit volume,  $q_a$ , from a layer  $k$  at a well is given by (Peaceman, 1983):

$$q_a = \frac{2p D z_k}{\ln \frac{r_{e,k}}{r_{w,k}} + s_k} \frac{k_e k_{ra}}{m_a} (p_k^w - p_k) \quad (5)$$

While temperature effects on relative permeability play a significant role in thermal simulations, we chose to neglect them in the current model. Thus, the influence of temperature in the simulation model is purely through changes in fluid viscosity and enthalpy.

### B. Sequential Formulation

The streamline method can be viewed as variant of sequential method. The idea of the sequential method is to separate an equation for the pressure from the component conservation equations. Assuming fluids and rock are incompressible and ignoring capillary pressure, we obtain the pressure equation by adding Eqs. (1) and (2):

$$\nabla \cdot k \cdot (\lambda_t \nabla p - \lambda_g \nabla D) = -q \quad (6)$$

The total mobility ( $\lambda_t$ ) and total gravity ( $\lambda_g$ ) are defined as:

$$\lambda_t = \sum_\alpha \frac{k_{r,\alpha}}{\mu_\alpha}, \quad \lambda_g = \sum_\alpha \frac{k_{r,\alpha} \rho_\alpha g}{\mu_\alpha}, \quad \alpha = w, o \quad (7)$$

The governing water saturation and energy transport equations for the sequential method can be derived from Eqs. (1) and (3). They take the form as:

$$\phi \frac{\partial S_w}{\partial t} + \nabla \cdot (f_w \bar{u}_t) + \nabla \cdot \bar{G}_w = f_w q_t \quad (8)$$

$$\phi \frac{\partial E}{\partial t} + \nabla \cdot (F \bar{u}_t) + \nabla \cdot \bar{G}_e = q_w \rho_w^w H_w^w + q_o \rho_o^w H_o^w \quad (9)$$

where

$$\bar{u}_t = -k \cdot (\lambda_r \nabla p - \lambda_g \nabla D) \quad (10)$$

$$f_\alpha = \frac{k_{r\alpha} / \mu_\alpha}{k_{rw} / \mu_w + k_{ro} / \mu_o} \quad (11)$$

$$E = S_w \rho_w U_w + S_o \rho_o U_o + \frac{1-\phi}{\phi} \rho_r C_r T \quad (12)$$

$$F = f_w \rho_w H_w + f_o \rho_o H_o \quad (13)$$

The gravity fractional terms for water equation ( $\bar{G}_w$ ) and energy equation ( $\bar{G}_e$ ) are defined as:

$$\bar{G}_w = k_z g \nabla D \gamma \quad (14)$$

$$\bar{G}_e = k_z g \nabla D \gamma (\rho_w H_w - \rho_o H_o) \quad (15)$$

where

$$\gamma = f_w \lambda_o (\rho_w - \rho_o) \quad (16)$$

### C. Streamline Formulation

Streamline simulation is greatly facilitated by the time-of-flight concept. Using the time of flight,  $t$ , as the coordinate space instead of the  $(x, y, z)$  coordinates, any 3D convection-driven equation can be transformed into multiple 1D equations that are solved along streamlines.

The time-of-flight can be expressed as:

$$\tau(x, y, z) = \int_0^s \frac{\phi}{|\bar{u}_t(s)|} ds \quad (17)$$

which is the time required to reach a distance  $s$  on a streamline based on the total velocity  $\bar{u}_t$  along the streamline. The permeability, porosity, and total mobility of the 3D domain are honored along the streamline by means of the  $\delta$  coordinate. To determine the coordinate transformation from  $(x, y, z)$  to  $t$ , rewrite Eq. 17 as:

$$|\bar{u}_t| \frac{\partial}{\partial s} = \phi \frac{\partial}{\partial \tau} \quad (18)$$

$|\bar{u}_t|$  can be expressed as:

$$|\bar{u}_t| = \frac{ds}{dt} = \frac{\partial s}{\partial x} \frac{\partial x}{\partial t} + \frac{\partial s}{\partial y} \frac{\partial y}{\partial t} + \frac{\partial s}{\partial z} \frac{\partial z}{\partial t} = \bar{u}_t \cdot \nabla s \quad (19)$$

Substituting Eq. (19) into Eq. (18) yields an expression for the operator equality on the streamline as:

$$\bar{u}_t \cdot \nabla = \phi \frac{\partial}{\partial \tau} \quad (20)$$

This equality is used to transform any convection-driven equations from a 3D problem to 1D problems on the streamlines.

Recognizing that  $\nabla \cdot \bar{u}_t = 0$  for incompressible flow and using Eq. (20), the governing sequential equations (Eqs. (8) and (9)) in the absence of a source/sink can be written as:

$$\frac{\partial S_w}{\partial t} + \frac{\partial f_w}{\partial \tau} + \frac{\nabla \cdot \bar{G}_w}{\phi} = 0 \quad (21)$$

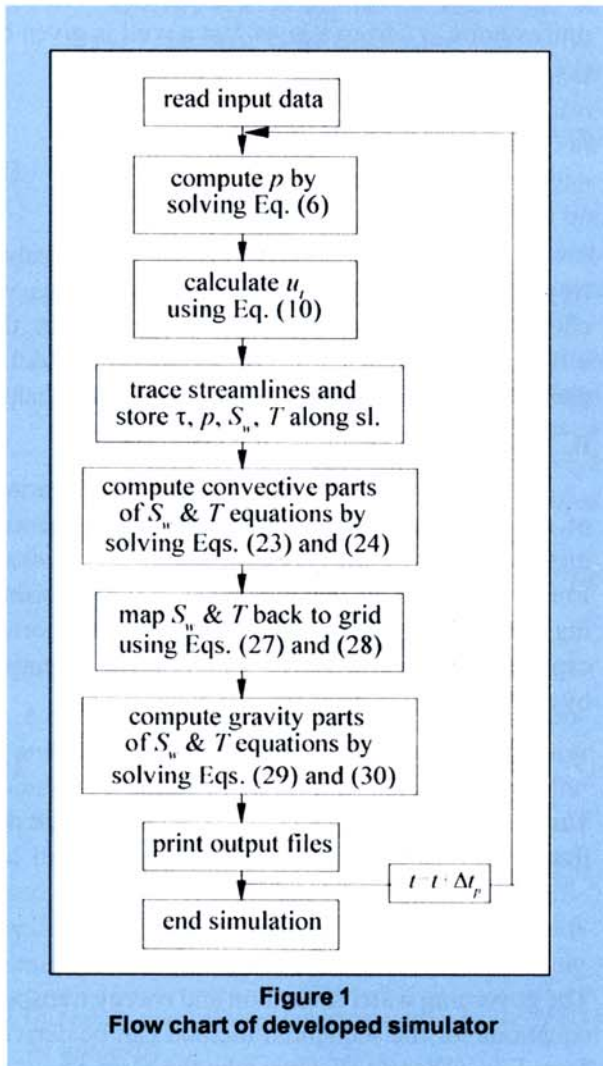


Figure 1  
Flow chart of developed simulator

$$\frac{\partial E}{\partial t} + \frac{\partial F}{\partial \tau} + \frac{\nabla \cdot \vec{G}_c}{\phi} = 0 \quad (22)$$

Eqs. (6), (21), and (22) form the governing set of nonlinear equations for the sequential method to be used in the streamline simulator. They are nonlinear since coefficients in each equation are dependent on the unknown variables ( $p, S_w, T$ ).

### III. SOLUTION PROCEDURE

A flow diagram of the solution procedure proposed here for the system governed by Eqs. (6), (21), and (22) is summarized in Figure 1. First, the governing pressure equation, Eq. (6), is solved by a standard finite difference scheme on the Cartesian grid with no-flow boundary conditions over the entire domain and a specified pressure or rate at the well equation, Eq. (5). Values of  $k_{ra}$  and  $m_a$  arising in the interblock transmissibility are taken from the phase upstream region. The wellbore mobility is assumed to be the gridblock mobility for production wells, and the injection phase mobility for injection wells. Once the pressure field is obtained, the total velocity field can be calculated using Eq. (10). Then, streamlines are traced by Pollock's approach (Pollock, 1988).

To solve Eqs. (21) and (22) in the sequential steps, the equations are split into two parts based on operator splitting. The convective parts are first solved along the streamlines and they are:

$$\frac{\partial S_w}{\partial t} + \frac{\partial f_w}{\partial \tau} = 0 \quad (23)$$

$$\frac{\partial E}{\partial t} + \frac{\partial F}{\partial \tau} = 0 \quad (24)$$

The above equations are solved simultaneously using the Newton-Raphson technique. The discretized forms in terms of their residuals:

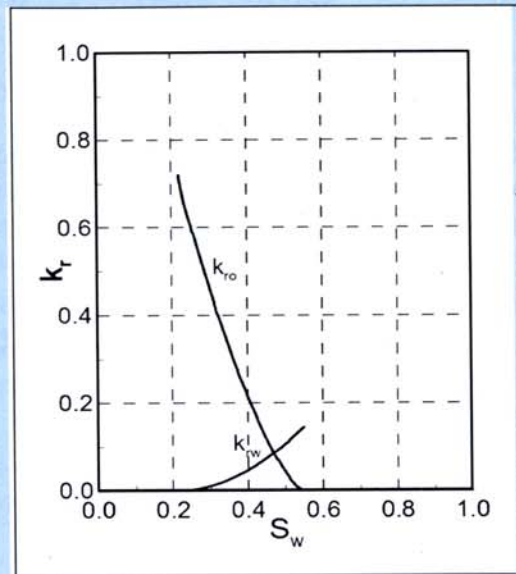


Figure 2  
Relative permeability curves

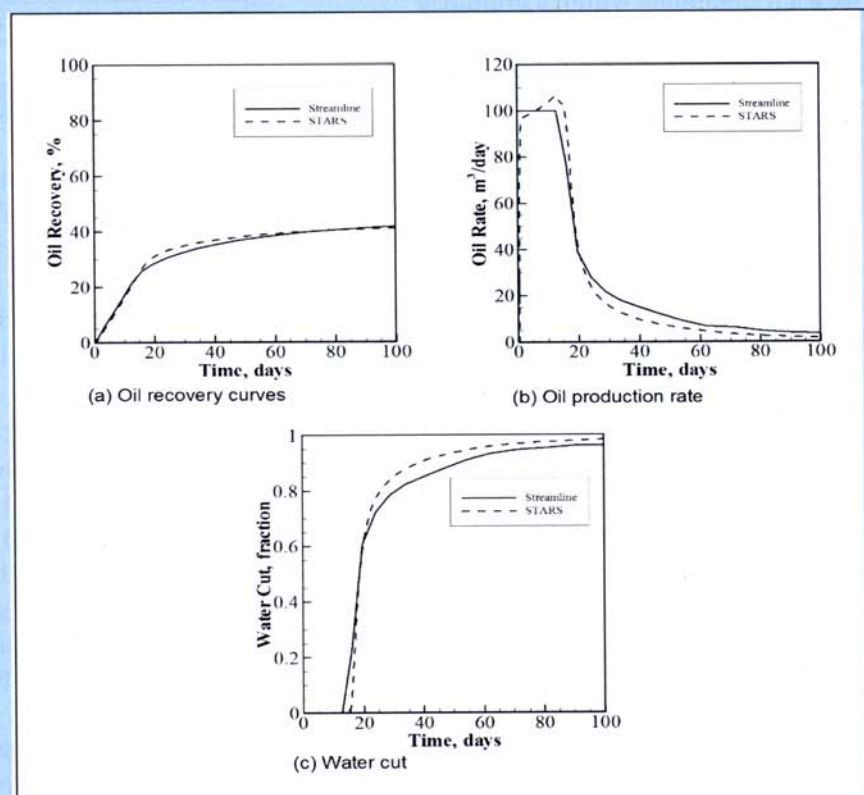


Figure 3  
Production performance of homogeneous case

$$R_S^c = \frac{1}{\Delta t} [S_{wi}^{k+1} - S_{wi}^n] + \frac{1}{\Delta \tau} [f_{wi+\frac{1}{2}}^{k+1} - f_{wi-\frac{1}{2}}^{k+1}] = 0 \quad (25)$$

$$R_T^c = \frac{1}{\Delta t} [T_i^{k+1} - T_i^n] + \frac{1}{\Delta \tau} [T_{i+\frac{1}{2}}^{k+1} - T_{i-\frac{1}{2}}^{k+1}] = 0 \quad (26)$$

where  $i$  represents nodes along a streamline,  $k$  and  $n$  denote Newton iteration level and pressure time level, respectively. The interblock quantities are evaluated by upstream weighting. After Eqs. (23) and (24) are solved, obtained are temporary  $S_w$  and  $T^c$  distributions along streamlines. These values are then mapped back to the gridblocks. The average  $S_w$  and  $T$  in a gridblock are defined as:

$$\bar{S}_w = \frac{\sum_{i=1}^{n_s} \Delta \tau_i S_{wi}}{\sum_{i=1}^{n_s} \Delta \tau_i} \quad (27)$$

$$\bar{T} = \frac{\sum_{i=1}^{n_s} \Delta \tau_i T_i}{\sum_{i=1}^{n_s} \Delta \tau_i} \quad (28)$$

where  $n_s$  is the number of streamlines in the gridblock. These weighting averages assume that the flux is the same for each streamline within a gridblock. Then, the gravity parts of Eqs. (21) and (22):

$$\frac{\partial S_w}{\partial t} + \frac{\nabla \cdot \vec{G}_w}{\phi} = 0 \quad (29)$$

$$\frac{\partial E}{\partial t} + \frac{\nabla \cdot \vec{G}_e}{\phi} = 0 \quad (30)$$

are solved simultaneously on the dimensional grid using and as the initial conditions. The discretized forms in terms of their residuals:

$$R_S^g = \frac{V_b}{\Delta t} [S_{wi}^{k+1} - S_{wi}^c] + \frac{1}{\phi} \left[ \left( \frac{A_z G_w}{\Delta z} \right)_{i+\frac{1}{2}}^{k+1} - \left( \frac{A_z G_w}{\Delta z} \right)_{i-\frac{1}{2}}^{k+1} \right] = 0 \quad (31)$$

$$R_T^g = \frac{V_b}{\Delta t} [T_i^{k+1} - T_i^c] + \frac{1}{\phi} \left[ \left( \frac{A_z G_e}{\Delta z} \right)_{i+\frac{1}{2}}^{k+1} - \left( \frac{A_z G_e}{\Delta z} \right)_{i-\frac{1}{2}}^{k+1} \right] = 0 \quad (32)$$

Table 1  
Fluid and rock properties

Parameters	Water	Oil
Density, kg/m <sup>3</sup>	993	900
Viscosity: $\mu = a_{vis} \cdot \exp(b_{vis} / T)$		
$a_{vis}$ , kPa·day	2.26213E-3	5.48901E-7
$b_{vis}$ , °K	1791.17755	5105.19253
Enthalpy, Internal Energy		
$C_g = c_1 + c_2 T + c_3 T^2 + c_4 T^3$ , $H_{vap} = h_{vap}(T_{cr} - T)^{c_{vap}}$		
$H_g = \int_{T_{ref}}^T C_g dT$ , $H_\alpha = H_g - H_{vap}$ , $U_\alpha = H_\alpha$		
$C_1$	32.24	-22.38
$C_2$	1.924E-3	1.939E+0
$C_3$	1.055E-5	-1.117E-3
$C_4$	-3.596E-9	2.528E-7
$h_{vap}$	25.1	287.1
$e_{vap}$	0.380	0.625
Initial water saturation, fraction		0.2175
Initial temperature, °C		32.2
Reservoir heat capacity ( $r_r C_r$ ), kJ/(m <sup>3</sup> ·°C)		2347
Porosity, fraction		0.3

It should be noted that when calculating the interblock transmissibility terms in the above equations, only the properties in the upstream side should be used. The iterative calculations for this gravity step tend to converge quickly. Our numerical experiments showed that the first approximation is sufficiently accurate.

The crucial point of numerical solution is the selection of the time step size. There are three different time steps here: (1) the time step elapsed between pressure updates, (2) the time step used in the convective step, and (3) the time step for the gravity step. As the temperature greatly affects the coefficients of the pressure equation, the calculation of pressure updates is controlled by the magnitude of the changes in temperature. This pressure time step size is also used for the gravity step. A practical rule was introduced to select the time step for the convective step. The typical values were found to be 0.2 to 1.0 times the pressure time step, which were obtained through the numerical experiments.

**IV. TESTS AND RESULTS**

In this section, we examine the validity of the proposed procedure. Several simulation results obtained by our model are compared with those by STARS.

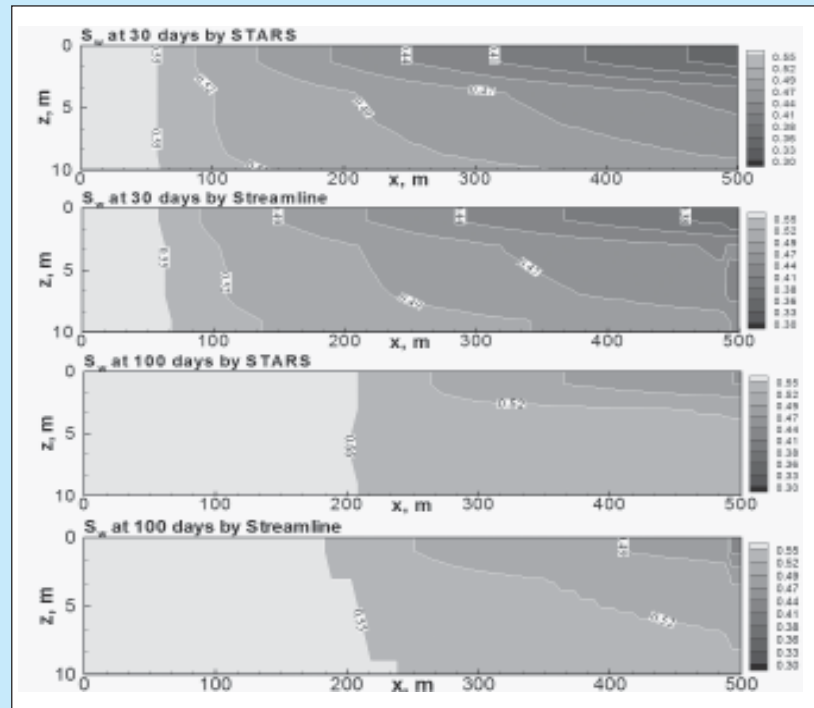
**A. Common Data**

Table 1 is a summary of fluid and rock properties data used for simulation. The relative permeability curves are shown in Figure 2. The wellbore radius is 0.09 m. The producer was constrained with bottom-hole pressure at 20700 kPa. The injector was constrained with rate at 100 m<sup>3</sup>/day cold water equivalent (CWE) with temperature of 150°C. The convergence criteria employed in Newton-Raphson's procedure are 0.02 for saturation and 5°C for temperature.

**B. Homogeneous case**

First we performed a simulation of hot waterflooding in a 2D vertical homogeneous reservoir of 3000 md. The dimensions were 500×5×10 m which was divided into 100×1×5 gridblocks. We ran the simulator for 100 days or the equivalent of 1.33 pore volume injected (PVI).

The production performance at the surface conditions obtained by streamline method is shown in Figures 3 (a), (b), and (c). For validation purpose, we have also shown the results from STARS. Comparisons of the water saturation profiles shown in Figure 4 provide insight into the reason



**Figure 4**  
Water saturation profiles for homogeneous case

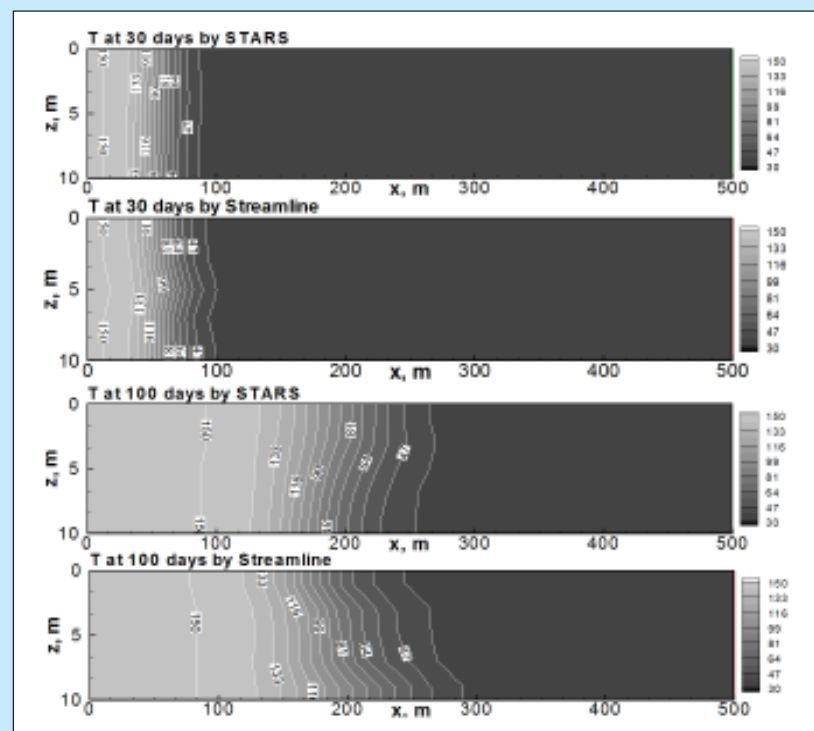


**Figure 5**  
Temperature profiles for homogeneous case

for the similarities and differences in the both simulation results. Much water has been produced by streamline simulation compared to STARS after 30 days injection as indicated by the 0.44 water saturation contours at the production layers. This explains earlier breakthrough of the water in streamline solution as observed in Figure 3c. After breakthrough, the water production became higher in STARS solution than streamline solution. This is consistent with the water saturation profiles. After 100 days injection, the 0.52 water saturation contour generated by STARS solution has taken place in the production layers higher than streamline solution. However, the corresponding recovery curves that represent the integrated response of the displacement are in good agreement between two simulators as can be seen in Figure 3a.

Note that the input water properties were adjusted by STARS in order to obtain the convergence solution. The water density was changed from 993 to 997 kg/m<sup>3</sup>, with the water compressibility factor and thermal expansion became 4.570E-07 kPa<sup>-1</sup> and 1.971E-04 °C<sup>-1</sup>, respectively. Effect of this water compressibility can be observed in the oil production rate profile in STARS solution. The oil production rate increases over 100 m<sup>3</sup>/day in the early period of simulation reflecting the system under compression, as shown in Figure 3(b). During this period, the streamline shows an oil production plateau of 100 m<sup>3</sup>/day which is the same as the total injection rate, indicating incompressible system.

Figure 5 compares the temperature fronts between two simulators. In the streamline solution, the temperature front move faster at the bottom of the reservoir rather than at the upper part of the reservoir as opposed to STARS solution. Knowing that

the water is denser than oil during the simulation period, the result of streamline solution likely supports our physical intuition. Water always flows downwards and oil always flows upwards causing gravity tongue at the bottom part of the reservoir.

To assess how well the operator splitting technique works for modeling gravity effects in the non-isothermal flow, the streamline simulation was run by turning off the gravity step. Figure 6 shows the water saturation and temperature profiles for this case. The gravity tongue was not developed, leading to what is known as piston-like displacement. But this does not represent the example studied here. Because of the difference between water and oil densities, the contours of equal temperature and water saturation are certainly not vertical within the reservoir. Thus, this test conformed that the mixed streamline and operator splitting techniques also work well for the non-

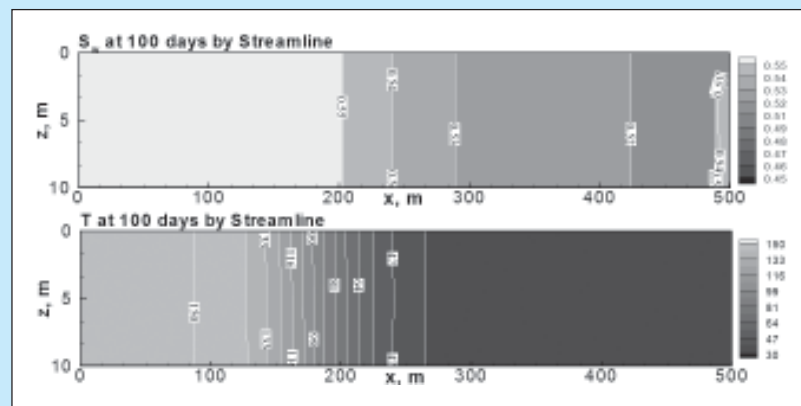


Figure 6  
Water saturation and temperature profiles generated by turning off gravity step

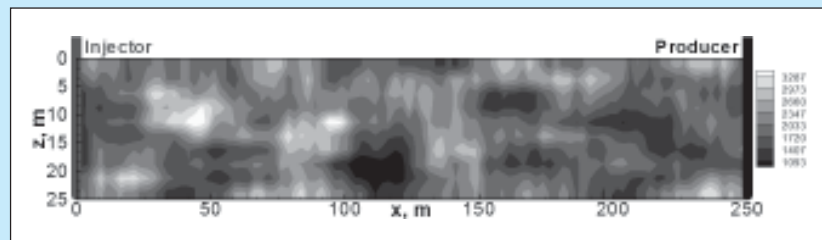


Figure 7  
Well locations and permeability distribution for heterogeneous case

isothermal problems. The underrunning of the water near the base of the reservoir is the result of the buoyancy forces between the water and the oil and is obviously significant.

### C. Heterogeneous case

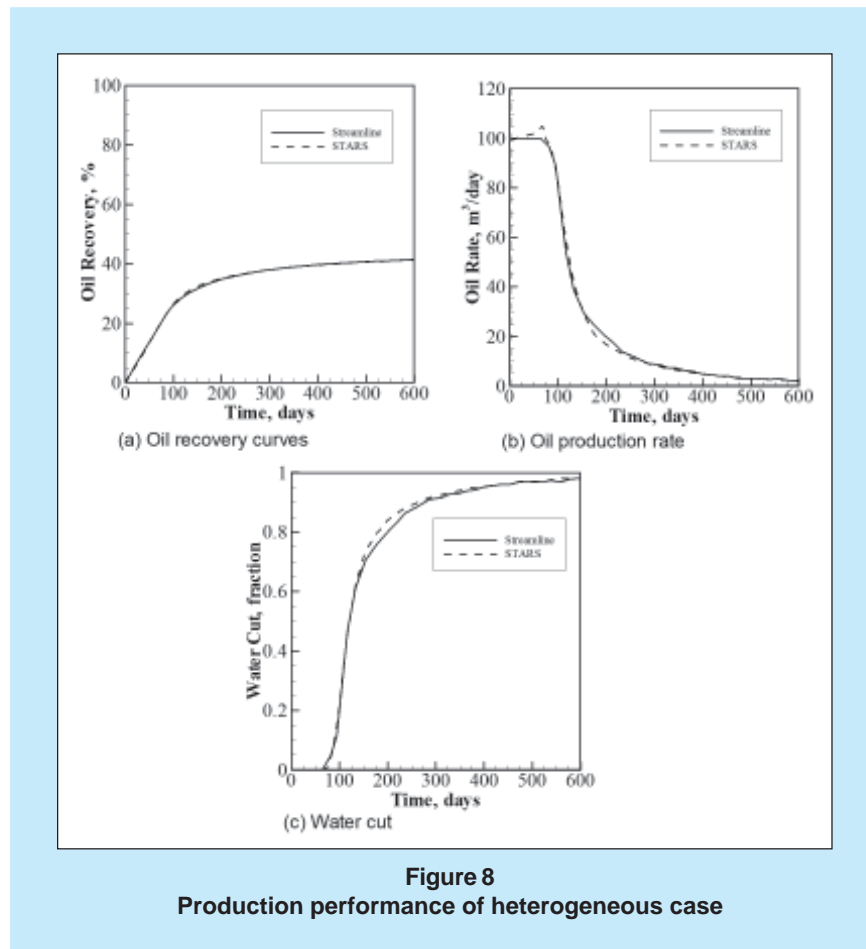
We next tested the proposed procedure in a heterogeneous reservoir. A 250×25×25 m reservoir was divided into 100×1×10 gridblocks. Figure 7 shows the well location and the permeability field. The values range from 788 to 3592 md as depicted by dark to light colors.

Figures 8(a)-(c) show the production performance for a total 600 days or 1.28 PVI. For validation purpose, we have also superimposed the results from STARS. There is very good agreement between streamline and STARS calculations. The same general behavior as the homogeneous case can be observed throughout the results of this case. As in homogeneous case, STARS adjusted the water properties in order to obtain the convergence solution. This results in different oil profile at early time between two simulators, as shown in Figure 8(b).

The water and temperature fronts are shown in Figures 9 and 10. The growth of the fronts shows visually what is taking place in the permeability model. The presence of a less permeable region at around 50 m in the *x*-direction and 20 m in the *y*-direction has retarded the water and temperature fronts. This pattern appears to be similar in the streamline and STARS solutions although there is more detail with high resolution in the streamline results.

### D. Model Run Time

Run time for the 100'1'5 homogeneous model with streamline was 0.23 min to reach 1.33 PVI, whereas STARS required 0.83 min. For the 100'1'10 heterogeneous model, streamline required 2.70 min to generate the solutions up to 1.28 PVI while STARS was 0.93 min. The inefficiency of streamline in this heterogeneous example mainly arises during the solu-



tion of 1D convective part. Abrupt changes in permeability caused the steep local changes of properties. As the stiffness of a system increases, more iteration is necessary for 1D solver to converge onto the solutions. We are currently pursuing the extension to decouple the 1D water and energy streamline equations and solve them separately. It will greatly reduce both the size of linear equation systems and the degree of nonlinearity, leading to improve the efficiency of 1D solver. However, because of the more frequent pressure recalculations to account for the high nonlinearity in the pressure equation for the non-isothermal problems, the speed up factor will be less compared to the isothermal cases.

### V. CONCLUSIONS

We developed the mixed streamline and operator splitting techniques to model gravity effects encountered in the non-isothermal flow. We have derived the coupled equations for streamline simulation of this problem and proposed a procedure to solve the equations. We tested the procedure for hot wa-

terflooding process in homogeneous and heterogeneous reservoirs. It was confirmed that the gravity step works well to model the buoyancy forces between water and oil. The results obtained by the developed model demonstrated acceptable comparison with the commercial thermal simulator.

A potential area of further work is to improve the numerical solutions of the mass and energy streamline equations in the sequential step. Also we have aims toward developing a tool for selection of the appropriate time step size to provide a basis for automatic control of time step within full field streamline simulations.

**VI. NOMENCULATURE**

- $A_z$  = cross section z-direction,  $m^2$
- $C_r$  = specific heat of rock,  $kJ/(kg \cdot ^\circ C)$
- $D$  = depth of gridblock from datum,  $m$
- $f_a$  = fractional flow of phase a, fraction
- $G_e$  = gravity fractional of energy,  $kJ \cdot m/(m^3 \cdot s)$
- $G_w$  = gravity component of water,  $m/s$
- $g$  = gravitational acceleration constant,  $m/s^2$
- $H_a$  = enthalpy of phase a,  $kJ/kg$
- $k$  = absolute permeability,  $m^2$
- $k_{ra}$  = relative permeability of phase a
- $n_s$  = number of streamline passed a gridblock
- $p$  = pressure,  $Pa$
- $q$  = volumetric flow rate,  $m^3/(s \cdot m^3)$
- $r_e$  = well drainage radius,  $m$
- $r_w$  = wellbore radius,  $m$
- $s$  = local streamline coordinate,  $m$

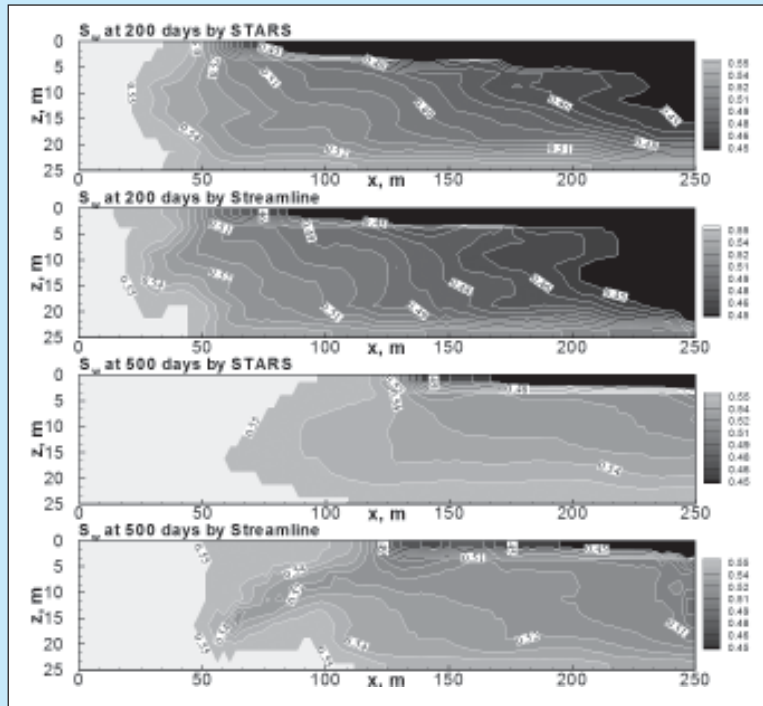


**Figure 9**  
Water saturation profiles for heterogeneous case

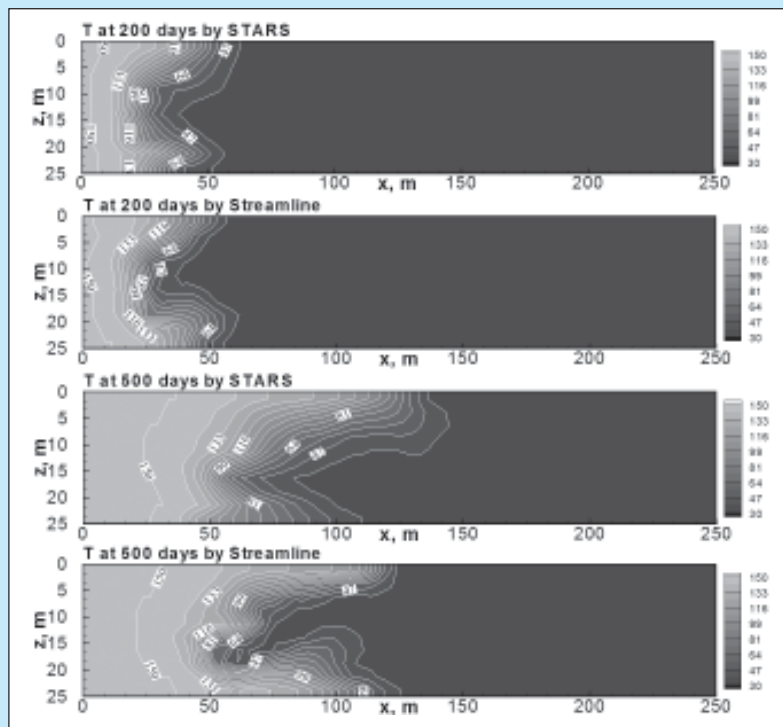


**Figure 10**  
Temperature profiles for heterogeneous case

$s_k$  = skin factor  
 $S_a$  = saturation of phase a, fraction  
 $T$  = temperature, °C  
 $t$  = time, s  
 $U_a$  = internal energy of phase a, kJ/kg  
 $u_t$  = total velocity, m/s  
 $u_a$  = velocity of phase a, m/s  
 $\Delta t$  = time step size, s  
 $\Delta z_k$  = gridblock dimension in z-direction, m  
 $\bar{e}_a$  = mobility of phase a, 1/(Pa·s)  
 $\bar{e}_t$  = total mobility, 1/(Pa·s)  
 $\bar{e}_g$  = total gravity mobility, 1/(m·s)  
 $i_a$  = viscosity of phase a, (Pa·s)  
 $\tilde{n}_r$  = rock density, kg/m<sup>3</sup>  
 $\tilde{n}_a$  = density of phase a, kg/m<sup>3</sup>  
 $t$  = time-of-flight, s  
 $f$  = porosity, fraction

#### Subscripts

$i$  = gridblock number  
 $S$  = saturation  
 $T$  = temperature  
 $t$  = total  
 $w$  = water

#### Superscripts

$c$  = convective step  
 $g$  = gravity step  
 $k$  = Newton iteration level  
 $n$  = pressure time level  
 $w$  = well

#### REFERENCES

1. Batycky, R., 1997, *A three-dimensional two-phase field scale streamline simulator*, PhD thesis, Stanford University.
2. Bratvedt, F. and Gimse, T. and Tegnander, C., 1996, Streamline computations for porous media flow including gravity: *Transport in Porous Media*, vol. 25, p.63-78.
3. Computer Modeling Group Limited, 2003, *STARS version 2003 User's Guide*, Calgary, Alberta Canada.
4. Crane, M., Bratvedt, F., Bratvedt, K., Childs, P. and Olufsen, R., 2000, A Fully Compositional Streamline Simulator: paper SPE 63156, In *Proc. the 2000 SPE Annual Technical Conference and Exhibition*, Texas, October 1-4.
5. Datta-Gupta, A. and King, M. J., 1995, A semianalytical approach to tracer flow modeling in heterogeneous permeable media: *Advances in Water Resources*, vol. 18, p.9-24.
6. Peaceman, D. W., 1983, Interpretation of well-block pressure in numerical reservoir simulation with nonsquare grid blocks and anisotropic permeability: *SPE Journal*, vol. 23, p.531-569.
7. Pollock, D. W., 1988, Semianalytical computation of path lines for finite difference methods: *Ground Water*, vol. 26, p.743-750.
8. Rodriguez, P.G., Segura, M.K. and Mustieles Moreno, F.J., 2003, Streamline methodology using an efficient operator splitting technique for accurate modeling of capillary and gravity effects: SPE 79693, In *Proc. the SPE Reservoir Simulation Symposium*, Texas, February 3-5.